MARS GLOBAL SURVEYOR MAPPING ORBIT DETERMINATION

Stuart Demcak[1], Pasquale B. Esposito, Darren T. Baird, Eric Graat

Jet Propulsion Laboratory, California Institute of Technology
4800 Oak Grove Drive
Pasadena, CA 91109-8099

Since the start of the mapping phase on March 9, 1999, the Mars Global Surveyor (MGS) spacecraft has been conducting an intensive global scientific study of Mars' surface, atmosphere and magnetic and gravitational fields. The MGS mapping orbit is polar, nearly circular, frozen, sun synchronous and has a period of 117.7 minutes, with a mean altitude of 402 km. The primary mission ends on February 1, 2001, at which time MGS will have completed 8505 orbits during one Mars year of mapping flight operations. Throughout this time, the navigation team has been responsible for providing the MGS engineering and science teams with spacecraft predicted and reconstructed ephemeris information. These were derived primarily by analyzing X-band Doppler tracking data. The methods and challenges of the orbit determination process are described in this paper.

The major challenges of the orbit determination have been the modeling of the Mars gravity field and the autonomous spacecraft angular momentum desaturations (AMDs). The Mars gravity field has been significantly improved over the last two years through the analysis of the MGS Doppler data. The AMDs have been frequent (three per day) and difficult to model. Furthermore, if not analyzed accurately, they can give rise to significant errors in the predicted time of future orbital events. For reconstruction analyses, each AMD has been individually analyzed in the orbit determination process. For prediction analyses, the AMDs are currently being modeled as an average perturbative acceleration. With respect to reconstruction, position errors are generally less than 10 m, 200 m and 3 m, respectively, in radial, down-track and cross-track. Where Doppler data is available, these errors reduce to 1 m, 50 m and 1 m, respectively. Typical equator crossing timing errors after seven days of prediction have been less than 3 seconds. However, any unexpected change in the character of the AMDs can increase these timing errors.

[1] OAO Corporation

NAVIGATION OVERVIEW OF MAPPING PHASE

The purpose of this paper is to present a detailed explanation of the MGS orbit determination (OD) process throughout the mapping orbit phase. In addition, we have investigated the major OD error sources and have assessed their impact on the accuracy of both reconstructed and predicted orbits.

After the completion of aerobraking, the initial mapping orbit was established with the transfer-to-mapping-orbit (TMO) propulsive maneuver, which was executed on 2/19/99 (Ref. 1). Thereafter, a seven-day interval was identified as a gravity calibration (GC) period, although two weeks prior to this time tracking data had also been acquired for GC. The purpose was to acquire continuous tracking data in order to refine the Martian global gravity field model in preparation for the mapping phase. Prior to this time, the most current gravity field model had been determined from tracking data acquired from three previous orbiters, namely, Mariner 9, Viking 1 and Viking 2. This model was a fiftieth degree and order gravity field referred to as Mars50c (Ref. 2). Initially, the navigation team updated this model based on the GC data. Throughout mapping, the radio science team has shared their interim gravity field models with us; currently, we are using their MGS75C gravity field model in our analysis (Ref. 3).

On 3/9/99, the MGS Project Manager announced the beginning of the mapping phase of flight operations. Based on science team preferences, an orbit counting convention was established whereby orbits were defined at descending equator crossings (DEQX). Osculating orbit elements and related parameters at the beginning of the mapping phase are given in Table 1; note that the nodal period was 117.7 minutes. The coordinate system is Mars centered, Mars mean equator of date and Earth mean equator of epoch J2000; LMST stands for local mean solar time.

Table 1

ORBIT ELEMENTS AT START OF MAPPING PHASE

Element	Periapsis Value	Apoapsis Value
Semi-major axis, km	3767.096	3767.541
Eccentricity	0.00548	0.0115
Inclination, deg	92.908	92.930
Arg of periapsis, deg	264.878	261.818
Long of ascend node, deg	7.971	7.995
Epoch, 3/9/99, ET	02:41:35	03:39:24
Period, minutes	117.0	117.02
LMST at DEQX, hr:min:s	02:02:46	

Because of an earlier problem associated with the deployment of the spacecraft's solar array (Ref. 4), several weeks of mapping flight operations were conducted in a fixed high gain antenna (HGA) mode. On 3/29/99, the HGA was successfully deployed and continuous data acquisition by all science instruments began in earnest (Ref. 5). During the mapping phase, only three orbit trim maneuvers (OTMs) were executed. Their purpose was to "trim-up" the frozen orbit parameters (Ref. 6) and adjust the orbit period in order to establish a more uniform distribution of ground tracks on Mars' surface. A summary of major events related to navigation is given in Table 2.

The nominal configuration of the spacecraft during mapping is given in Figure 1 with the +Z spacecraft axis pointed in the nadir direction as maintained by the on-board horizon sensor assembly. The spacecraft's configuration, orientation and self-induced forces, especially angular momentum desaturations (AMDs), are inextricably bound to the navigation process. In particular, AMDs are essentially small velocity changes, similar to small propulsive maneuvers, and cause orbital perturbations which must be accounted for in the orbit determination process. The analysis and evaluation of these frequent AMDs are important in both the orbital reconstruction and prediction processes and shall be covered in detail in the following sections.

Table 2

MAPPING PHASE MAJOR NAVIGATION EVENTS

Event	Date	Comment
Gravity calibration	02/04-26/99	Refine Mars gravity model
Start mapping mission	03/09/99	DEQX orbit convention
Deploy HGA (orbit 247)	03/29/99	Frequent attitude control thrusting
MGS in contingency mode	04/16/99	Azimuth gimbal motion restriction
OTM-1 (orbit 729)	05/07/99	ΔV = 3.54 m/s; adjust orbit*
OTM-2 (orbit 1144)	06/10/99	ΔV = 0.18 m/s; adjust orbit
OTM-3 (orbit 1905)	08/11/99	ΔV = 0.37 m/s; adjust orbit
Start beta supplement mode	02/07/00	Earth beta angle = 43 deg
Mars superior conjunction	07/01/00	Restricted commanding
Edge-on orbit configuration	12/15/00	Earth beta angle is zero deg
End primary mission	02/01/01	Orbit 8505 (694.9 days)

* ΔV = delta-velocity or magnitude of the velocity change maneuver.

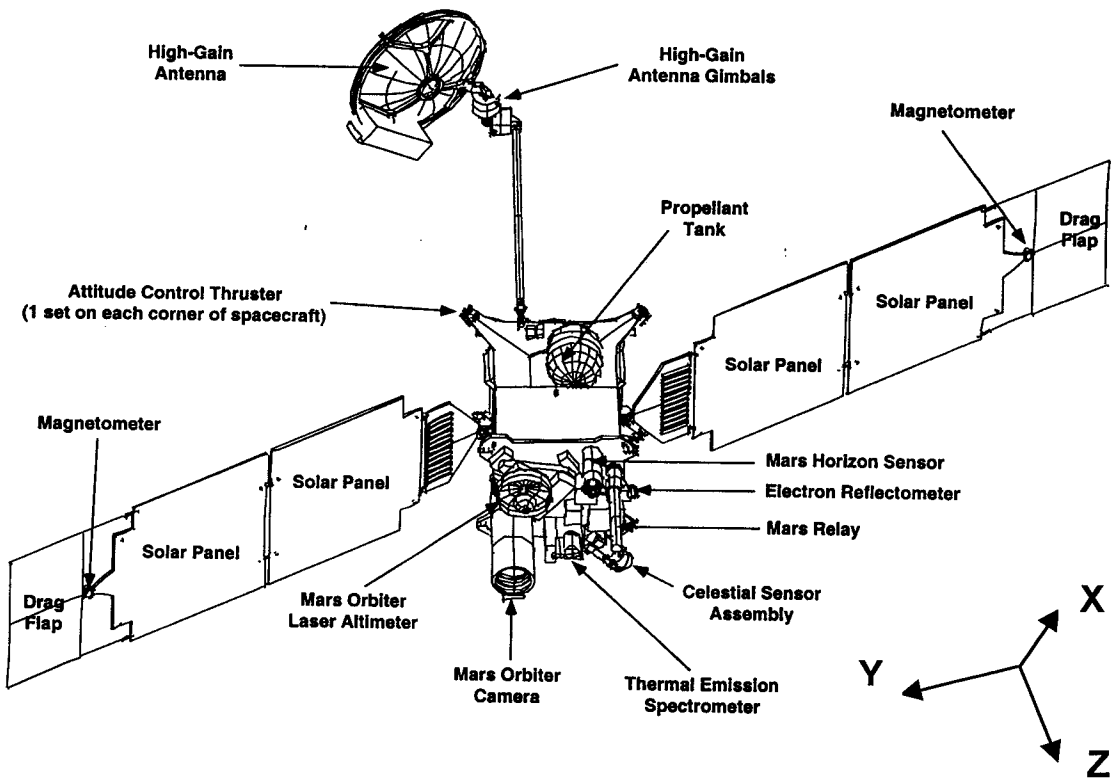

Spacecraft Axes

Z: nadir direction (toward Mars)

Y: along solar array or orbit angular momentum

X: completes right hand coordinate system (toward reader; opposite the spacecraft velocity)

Figure 1 MGS Spacecraft In The Mapping Configuration

On April 16,1999, the spacecraft experienced an anomaly whereby the azimuthal motion of the HGA was unexpectedly obstructed. The spacecraft's flight software and fault protection logic commanded MGS into a protective mode called "contingency" until Lockheed Martin Astronautics (LMA) flight engineers could analyze and resolve the problem. Because of the restricted HGA motion, a new mode of spacecraft operations was developed called beta supplement (Ref. 7). This operational mode started on 2/7/00 and shall continue until 6/19/01 when the Earth beta angle, effectively, the angle between the orbit plane and the direction to Earth, exceeds 43 degrees.

NAVIGATION MODELS

This section presents a description of the orbit determination models used for mapping operations. These models can be divided into two broad categories: dynamic and observable. Dynamic models are those which affect the translational motion of the spacecraft. The dynamic models include the Mars gravity field, spacecraft attitude and solar radiation pressure, and thruster activity. The observable models are those which change the path length of the tracking signal, such as two-way time delay or range and Doppler shift. The observable models comprise the signal path environment and station transmitter and spacecraft transponder biases and delays.

A 75th degree and order spherical harmonic Mars gravity field model, identified as MGS75C, truncated to 55x55 is employed in the orbit determination process. MGS75C was developed by the MGS radio science team and is based upon analysis of one-way, two-way and three-way Doppler and range tracking data. These data were acquired during the science phasing orbits, gravity calibration orbits and the mapping phase until 11/08/99. Navigation utilizes the IAU 1991 definition of the Mars astrodynamic constants, and the MGS75C model is consistent with these constants as well. In addition, we use the USGS Mars reference spheroid (a = 3393.4 km and f = 0.0052083) and the JPL planet and Mars satellite ephemerides DE405 and MAR033, respectively (Ref. 8). Since the MGS altitude averages 402 km and we analyze only short data arcs (3 to 22 orbits), no Mars atmospheric model is included in our orbit determination process.

For the mapping mission, we have modeled the spacecraft's attitude in spacecraft coordinates, as defined in Figure 1. To account for solar radiation pressure (SRP), the spacecraft is modeled using a collection of five flat plates and a parabolic dish. These components can be oriented with respect to the Sun independently or in groups. The area, specular reflectivity (μ) and diffuse reflectivity (ν) of each component have been calculated from information supplied by LMA. Table 3 summarizes the physical properties of these components. The HGA is modeled by the parabolic dish which points towards the Earth during each mapping orbit. Next, two flat plates are used to model the solar power array assembly (SA1 and SA2). The orientation of the solar power array undergoes a sequence of discrete changes during each orbit. We model these discrete changes using information extracted from the mapping sequence of events files. Lastly, the three remaining flat plates are affixed to the spacecraft +X, +Y and +Z axes to model the equipment bus (see Figure 1).

MGS maintains attitude with the aid of three reaction wheels, each oriented along the spacecraft axes. The reaction wheels build up angular momentum to counter the torques induced by solar radiation pressure and gravity gradient effects. The accumulated angular momentum is removed autonomously from the wheels via a pair of 4.45 N thruster firings. The larger AMD events, the spin-axis AMDs, occur approximately every 7.5 hours, imparting a velocity change ranging between 13 - 22 mm/s along the spacecraft +Z axis. The less significant AMD events, the yaw-axis AMDs, occur at approximately 30-hour intervals and impart a velocity change of less than 1.0 mm/s. The AMD thruster activity usually occurs over a period of 3 to 4 minutes. Each AMD event is composed of a series of short sub-second pulses separated by longer periods of inactivity. The "pulse-width" is 0.09 seconds for the spin-axis AMDs and 0.067 seconds for the yaw-axis AMDs. The "dead time" between pulses is 7.91 seconds. There are between 20 to 40 pulses per AMD event. From the daily replay of engineering telemetry, the AACS team provides navigation with a reconstruction of these AMD events via a formatted text file. The data on these

files include the start and end times of the AMD, the spacecraft attitude, what thrusters were active and the impulse imparted by each active thruster. There is a latency of 1.5 to 2.5 days in the delivery of the AMD files to the Navigation Team (Nav).

Table 3

MGS SRP MODEL PARAMETERS

Component	μ	ν	Dimensions
HGA	0.000	0.293	Radius: 0.75 m Depth: 0.26 m
SA 1	0.173	0.096	8.139 m^2
SA 2	0.173	0.096	8.139 m^2
+X Bus	0.000	0.293	3.594 m^2
+Y Bus	0.000	0.293	3.594 m^2
+Z Bus	0.000	0.293	2.945 m^2

The AMD files are input directly to the JPL navigation software, which outputs a position and velocity change to the spacecraft center of mass at the end time of each event. Navigation regularly solves for, or updates, the velocity components of the reconstructed AMDs. Two significant discrepancies have been observed between the LMA reconstruction and the navigation estimates of the AMD events. First, the velocity change magnitude in the LMA reconstruction is approximately 20 percent greater than that observed in the analysis of the tracking data. Second, and more significant to the ability to predict the future trajectory, a velocity component along the spacecraft X-axis between 0.1 - 3.0 mm/s has been observed. This anomalous velocity component is primarily due to thruster plume impingement on the HGA assembly.

Small corrections to the Doppler and range observable models are required for accurate orbit determination. Signal path deviations due to the Earth's ionosphere and troposphere are applied in the orbit determination process with model updates occuring once per week. Information providing corrections to the Earth rotation and pole orientation are updated twice each week. The one-way Doppler tracking data from the ultra-stable oscillator (USO) exhibits a bias of nearly -4.9 kHz for an X-band transmitter frequency of approximately 8.4 GHz. Orbit solutions utilizing the USO one-way Doppler data must account for this bias. The range data require a 784.25 ns (235.11 m) or 794.50 ns (238.19 m) correction to account for the separate delays in the spacecraft's two X-band transponders.

NAVIGATION STRATEGY

The orbit determination filter configuration for mapping operations uses a single batch, weighted least squares, square-root information algorithm. The tracking data used for each orbit solution consists of X-band Doppler data collected at 10-second samples over several orbits (3 to 4 for prediction analyses and 17 to 22 for reconstruction analyses). Plans for mapping operations originally called for Deep Space Network (DSN) coverage of one 10-hour tracking pass per day with an additional pass every third day. The actual tracking of MGS has increased beyond the planned coverage, often reaching 16 hours per day during the beta supplement operations. Tracking data quality is typically better than 0.08 mm/s for the one-way, two-way and three-way Doppler data. This USO one-way Doppler data can be included in an orbit solution when two-way Doppler data are available to resolve the bias previously mentioned. Typically, around 10 percent of the tracking data have been one-way Doppler, although there have been periods of time where over 50 percent were one-way data. The two-way Doppler coverage has been sufficient to permit the ulitization of the majority of the one-way data. The parameters estimated in an orbit solution include the spacecraft epoch state (position and velocity), a subset of the gravity field coefficients, the three

velocity components of any AMD events occuring within the data arc and terms for the USO transmitter frequency bias and rate. Table 4 summarizes the a priori uncertainties of the estimated parameters.

Table 4

FILTER A PRIORI MODEL UNCERTAINTIES

Parameter	A Priori Uncertainty (1-sigma)
State: X, Y, Z (km)	100, 100, 100
ΔX, ΔY, ΔZ (m/s)	10, 10, 10
One-way Doppler bias (Hz)	1.0 - 10.0
One-way Doppler rate (Hz/s)	$10^{-8} - 10^{-6}$
Gravity Coefficients	
J6, ...,J15; C,S7,..., C,S13	30 times the formal MGS75C uncertainties
Spin AMD: ΔVx, ΔVy, ΔVz (mm/s)	3.0, 0.6, 10.0
Yaw AMD: ΔVx, ΔVy, ΔVz (mm/s)	0.3, 0.3, 0.3

ORBIT DETERMINATION AND RESULTS

Throughout mapping, the navigation team is responsible for predicting the orbit evolution of the spacecraft for at least 20 days and accurately reconstructing the orbits for the previous week. A reconstruction analysis consists of fitting tracking data in 17 - 22 orbit batches while accurately modeling all forces acting on the spacecraft. During a prediction analysis, 3 - 4 orbits of data are analyzed, but AMD information is not available. Thus, AMDs must be estimated for both amplitude and epoch and refined until a minimum sum of squares of Doppler data residuals is established.

Real-time tracking data are obtained directly from the DSN and displayed and formatted by the Automated Radiometric Data Validation and Real-time Correction (ARDVARC) program. ARDVARC decodes raw DSN data to create the Doppler data observables. These observables are subsequently validated and time ordered in a binary file for input to the navigation software. Also, a NASA Communication (NASCOM) file can be updated and read directly by ARDVARC. The NASCOM file allows Nav to monitor the data residuals as well as permits data to be archived for future processing.

Reconstructed Orbital Analysis

Approximately 17 - 22 orbits of data are analyzed or fit for a reconstruction solution. With MGS in a nearly 2-hour, circular orbit, approximately 34 – 44 hours of data are analyzed for each orbit batch. The solution batch is selected so that the first and last orbits analyzed have adequate tracking coverage (i.e. all orbits not tracked are bracketed by orbits that are tracked). This strategy helps to minimize the spacecraft's position error.

The final reconstruction product is created by merging the results from three to five analyses conducted over the course of a week. After all the known external forces are accounted for, the observed USO one-way, two-way, and three-way coherent Doppler residuals are analyzed, and suspect data points are removed from the fit. Suspect tracking data may be caused by AMDs, charged particle effects, spacecraft attitude changes, HGA motion due to solar panel orientation changes, and the effects of the Martian atmosphere as the spacecraft enters and exits occultation. When the properly edited data are correctly weighted, the end results are residuals that have a zero mean and contain a random distribution. Typical peak-to-peak post-fit residuals are generally within 20 mHz throughout the data arc. Typical pre-fit residuals, in contrast, display significant structure, often starting within 0.1 Hz and increasing throughout the data arc to 100 Hz. Representative pre-fit and post-fit Doppler residual plots will be presented in the following section on AMDs.

The accuracies of the spacecraft position are less than 50 m where Doppler data are available and increase to 200 m where no data exist. The formal spacecraft position and velocity uncertainties resulting from a typical reconstruction analysis are 10 m in the root sum square (RSS) position and 3 mm/s in RSS velocity. By comparing our reconstruction analyses with results from the radio science team and internal comparisons with overlapping trajectories, downtrack position errors have been shown to be typically less than 200 m, while radial errors are less than 10 m and crosstrack errors are generally less than 3 m. Where Doppler data are available, these errors are typically 50 m, 1 m and 1 m in down-track, radial and cross-track. These errors were degraded during the special egde-on orbital geomety.

Predicted Orbital Analysis

Three to four orbits of tracking data are analyzed during each prediction. The quality of the prediction deteriorates with less than two orbits of data. Because AMDs occur, on average, once every 7.5 hours, no more than four orbits of data (eight hours) are fit to avoid the possibility of two AMDs occurring during the data arc. Using these three to four orbits of fit data, 20-day predicted spacecraft ephemerides are distributed for use by the sequence, science, and DSN teams. As of September 2000, 180-day predictions are constructed each month to guide the science teams with future planning strategies.

An initial analysis is used to determine if any structure or signature exists in the data residuals, which could indicate the presence of an AMD or another dynamic modeling error. Once the epoch of the AMD is determined, as described in the next section, a velocity perturbation model is used to account for the AMD ΔV. Subsequently, the data are edited to remove suspect data, and the trajectory is integrated for 20 days. The Z component of acceleration (nadir direction) due to AMDs contributes little to the descending equator crossing time error, but the down-track component induces a noticeable timing error. Therefore, an average acceleration model is incorporated into the integrator that accounts for the influence of future AMDs. A constant acceleration of 5.93E-10 km/s^2 in the Z direction and –3.50E-11 km/s^2 in the X direction (down-track) is currently used to model the equivalent average velocities of 16 mm/s and -0.945 mm/s, respectively, once every 7.5 hours. The acceleration model has evolved since its inception and is updated to generate high quality predictions for use in image selection or targeting. Table 5 shows the evolution of the acceleration from its inception through the present time.

Table 5

EVOLUTION OF PREDICTION ACCELERATION MODEL (10^{-10} km/s^2)

Starting Date	X Component	Z Component
06/11/2000	-0.050	0.00
09/07/2000	-0.250	5.93
10/12/2000	-0.278	5.93
11/16/2000	-0.300	5.93
12/11/2000	-0.325	5.93
01/04/2001	-0.350	5.93

Generally, our prediction of the descending equator crossing time is accurate to within 20 seconds over 20 days. Timing errors greater than 20 seconds have been noticed but are not common. Typical position errors after 20 days are less than 0.2 km, 70 km and 0.04 km, respectively, in the radial, down-track and cross-track directions. Prediction accuracies are determined by differencing, for example, the descending equator crossing times from those generated by the reconstruction analysis, which is considered to be the truth (typically accurate to 0.002 - 0.06 seconds).

During solar conjunction, the ability to predict the descending equator crossing time was hindered by excessive noise caused when the signal transmitted by the DSN antennas passed through the charged particles of the solar corona. Therefore, analysis was performed before solar conjunction to establish a

baseline of descending equator crossing time errors for long-term accuracy (45 days). Table 6 shows the descending equator crossing time errors between the predicted and reconstructed trajectories after 3, 5, and 20 days for four cases that occurred before solar conjunction. No acceleration model was incorporated into these orbit predictions because the effect of AMDs was minor on the orbit prediction models.

Table 6

DESCENDING EQUATOR CROSSING TIME ERRORS (SECONDS)

Epoch	After 3 days	After 5 days	After 20 days
09/23/1999	-0.17	-0.11	9.0
11/11/1999	0.18	0.09	-8.0
12/29/1999	1.11	2.39	22.5
03/02/2000	0.32	0.51	-1.8

AMD ΔV variations cause small positive and negative changes to the orbit period, and the resulting timing errors can change direction (sign) accordingly. This effect can be seen in the timing errors of the 09/23/1999 and 11/11/1999 cases in Table 6. More information on the effects of AMDs will be presented in the next section. Other force models and their associated errors, such as solar radiation and atmospheric drag, were examined and found to produce negligible errors.

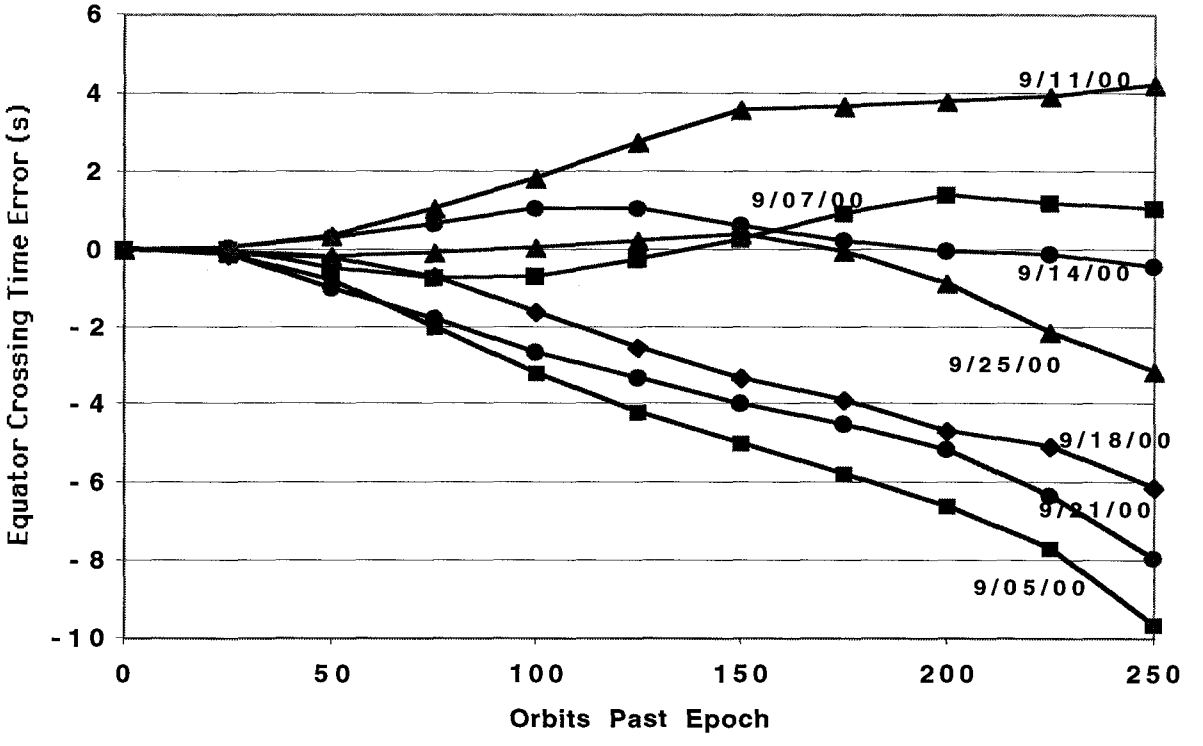

Figure 2 Descending Equator Crossing Time Error Propagation

By September 2000, after solar conjunction, high quality tracking data were being acquired by the DSN, and an accurate acceleration model was incorporated into the analysis to account for the velocity changes imparted by the AMDs. Figure 2 shows the descending equator crossing time error over 250 orbits for seven prediction analyses performed throughout September 2000.

During September 2000, the incorporation of an acceleration model into the predictions allowed the Nav team to predict the descending equator crossing time errors to within 10 seconds over 250 orbits. In fact, the 9/14/2000 prediction was superb as the descending crossing time was predicted to within 1 second over 3 weeks. This excellent prediction capability is highly dependent on consistent AMD behavior and is, therefore, not typical. Nevertheless, using an average acceleration model to account for future AMDs has allowed us to perform more accurate orbit determination than would otherwise be possible.

ANGULAR MOMENTUM DESATURATIONS: EVALUATION AND ERROR

The most significant error source in the orbit determination process is the modeling of AMD events. There are three methods for deriving these models, depending on the analysis strategy and a priori AMD information. First, in a reconstruction analysis, a priori AMD models are generated from AMD files provided by the SCT. The Doppler data are then used to refine these models. Second, in a prediction analysis, all AMD information must be deduced from the Doppler data. The third and most difficult case is the modeling of future AMDs. They are modeled as a constant acceleration derived from the recent average effect of the AMDs on the spacecraft trajectory. Each of these methods shall be described in detail.

AMD Evaluation for Reconstruction

A priori AMD information is critical to the reconstruction analyses. The AMD files provide accurate execution times along with less accurate ΔV information. Since it is difficult for Nav to determine AMD times to within 1 minute, Nav relies on the AMD files for this information. Accurate ΔV's can then be derived from the Doppler data and result in ΔV improvements of up to 40 percent. Figure 3 shows the Doppler residuals for a typical reconstruction OD solution. There are five spin-axis AMDs within this data arc, which occur at the following times (hr:min, Earth receive time, in time order): 13:10, 19:47; 04:25, 12:34, 19:30. If this solution is repeated with no AMDs modeled (Figure 4), the standard deviation of the Doppler residuals increases from 4.8 mHz to 120 mHz. 1 Hz is equivalent to 17.8 mm/s for two-way Doppler and 35.6 mm/s for one-way Doppler. There have only been a few cases when AMD information from the spacecraft was permanently lost. The most significant losses occurred during a spacecraft contingency mode and during solar conjunction. In these cases Nav could not reconstruct the AMD information, resulting in degraded reconstruction accuracies and poor Doppler residuals similar to Figure 4.

AMD Evaluation for Prediction

Since current Doppler data are used in a prediction analysis, AMD information is not yet available from the Spacecraft Team (SCT). Although only three orbits are typically analyzed, there usually is an AMD in the Doppler data arc. This causes the Doppler residuals to be very poor until an accurate AMD model can be derived. Determining this AMD is a lengthy process and significantly complicates the prediction analysis.

Several strategies can be used to determine the epoch of an AMD to within a minute. In the case where the AMD is not directly observable in the Doppler residuals, the analyst will have to fit subsets of the Doppler data to narrow the time interval in which the AMD must occur. If this time interval is within a data gap, additional solutions must be performed by varying the AMD execution epoch and estimating its ΔV. The accuracy of the AMD model is determined by examining the Doppler residuals and the estimated ΔV. Most of the ΔV should be along the spacecraft Z-axis, with only a small component of no more than 4 mm/s in the X direction. The Y component is generally less than 1 mm/s.

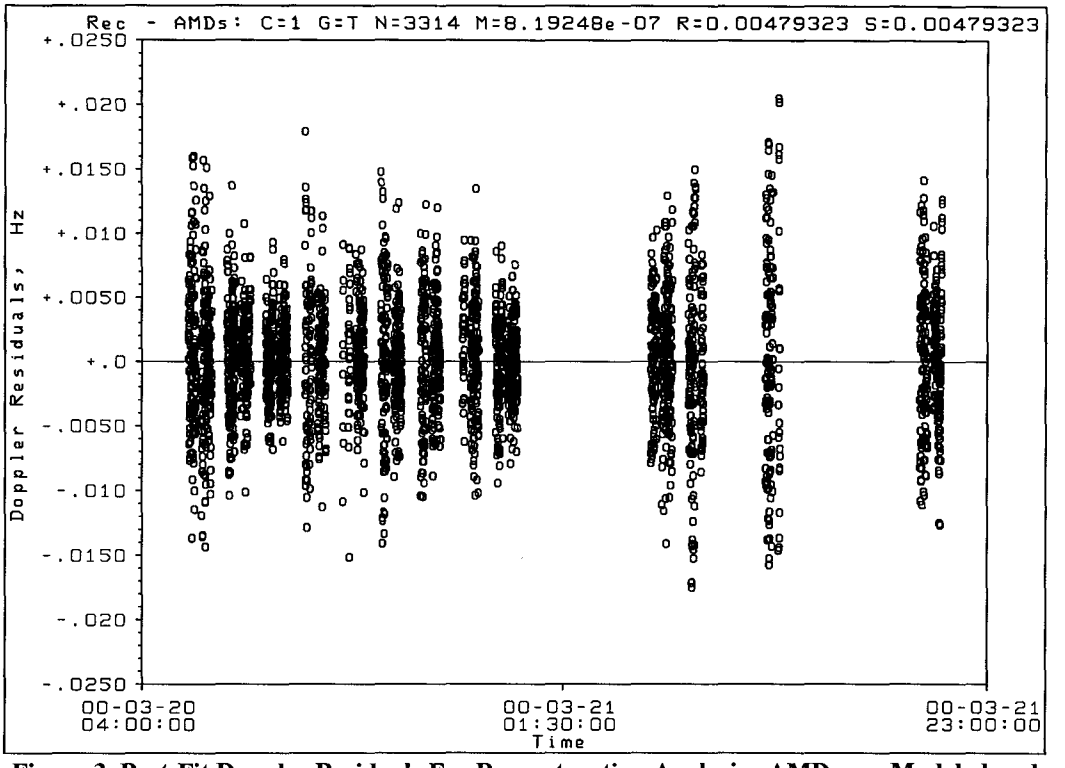

Figure 3 Post-Fit Doppler Residuals For Reconstruction Analysis. AMDs are Modeled and Estimated.

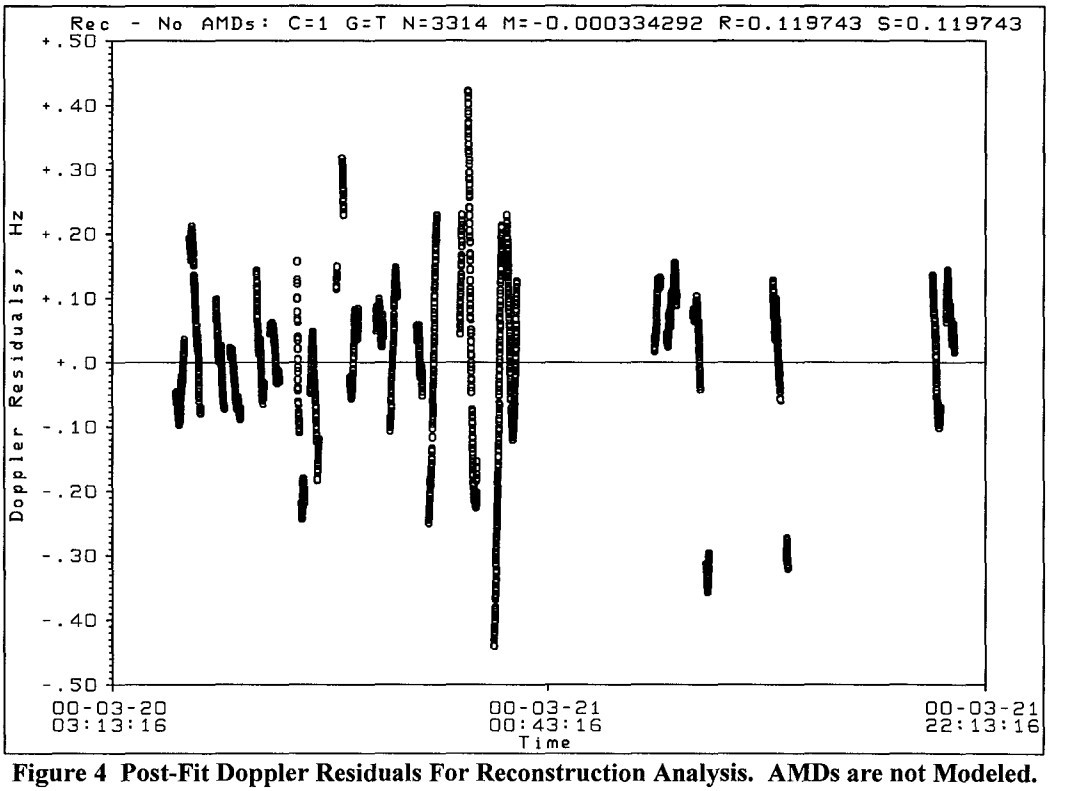

Figure 4 Post-Fit Doppler Residuals For Reconstruction Analysis. AMDs are not Modeled.

An understanding of how the AMD ΔV is manifested in the tracking data is also important in reconstructing an AMD event. Doppler measures the relative velocity projected along the Earth-spacecraft or line-of-sight (LOS) vector. Therefore, the orientation of the AMD ΔV with respect to the LOS determines how much of the AMD effect is contained in the surrounding Doppler data. If an unmodeled AMD occurs within a continuous span of Doppler data and has a ΔV parallel to the LOS, it will be directly observable in the Doppler residuals as a large signature. An accurate epoch for the AMD can then be immediately determined. On the other hand, if it is perpendicular to the LOS, it may be undetectable in the surrounding residuals. It will have the indirect effect, though, of degrading the residuals throughout the fit region. If the AMD occurs within a data gap a similar effect will be seen.

Although an unmodeled AMD is not always directly observable in the Doppler residuals, it is easily observed in range residuals. Although the range data are not fit, they can be passed through the Doppler only solution to generate range residuals. An AMD effect appears as a constant offset in the range residuals, enabling the analyst to reduce the time interval within which an AMD may occur. Once an AMD is modeled, an error in its epoch will also appear as a constant offset in the range residuals. Due to project priorities, telecommunication link degradation and orbit constraints, range data has only been available during part of the mapping phase. When available, there should be at least five range data per orbit with an accuracy of less than 3 m. Biases in the range data can also complicate AMD determinations, especially during DSN station handovers. Range data were periodically available up until the start of beta supplement (2/7/00), at which time accurate gravity fields were available. The improved gravity models made it easier to locate AMDs with Doppler-only data analyses.

Throughout the OD process, outlier Doppler data, as described in the Reconstructed Orbital Analysis section, must be removed. However, the degradation of the initial fit due to the unmodeled AMD makes it difficult to detect many of these data. If the inaccurate Doppler data are kept in the solution they can partially mask AMD effects. Furthermore, the unmodeled AMD can cause some good Doppler data to initially appear to be outliers. Fits of sub-arcs of the data which do not contain an AMD can be useful in the determination of outliers. Removal of suspect data is an ongoing process which requires the reevaluation of the Doppler residuals after each solution.

Prediction Analysis Example

The prediction OD analysis procedure can be clarified by stepping through the March 20, 2000 analysis (Figures 5 through 9). Four orbits of one-way and two-way Doppler data were fit. No range data were available to aid in the search for an AMD. The initial spacecraft epoch state was derived by propagating the trajectory from the previous analysis on March 16. The nominal gravity field was MGS75C. Figure 5 shows the initial pre-fit Doppler data residuals and demonstrates the accuracy of the a priori modeling. As expected, these residuals are very poor. The plot header shows several numerical quantities describing the quality of the fit, such as the number of data points (N=1037) and the standard deviation or "sigma" on the Doppler residuals (S=6981 mHz). The large data gaps are due to geocentric occultations while the short data gaps are from the high gain antenna motion constraints in beta supplement mode.

The first solution assumes that no AMD exists in the data arc. The resulting Doppler residuals (Figure 6, sigma of 10.7 mHz) have decreased significantly from the pre-fit residuals. However, the sigma on the residuals is a factor of three larger than desired and shows significant structure. Therefore, it appears that an AMD exists some place within this data arc. The residuals show no obvious place where an AMD may exist, so the next step is to fit subsets of Doppler data, also using this opportunity to remove additional Doppler outliers. Figure 7 shows the Doppler residuals when only the first two orbits are fit. They are small with no significant structure, and the sigma of 4.3 mHz is close to the value expected from a good fit. A similar solution fitting the last two orbits also shows good Doppler residuals. Therefore, it appears that the AMD is somewhere during the Earth occultation between the second and third orbit. Several solutions are generated, estimating for a ΔV modeled at different times within the occultation. The Doppler residuals

for the best solution (Figure 8, sigma of 5.9 mHz) are still large and have significant structure, which implies that the AMD does not occur during the occultation.

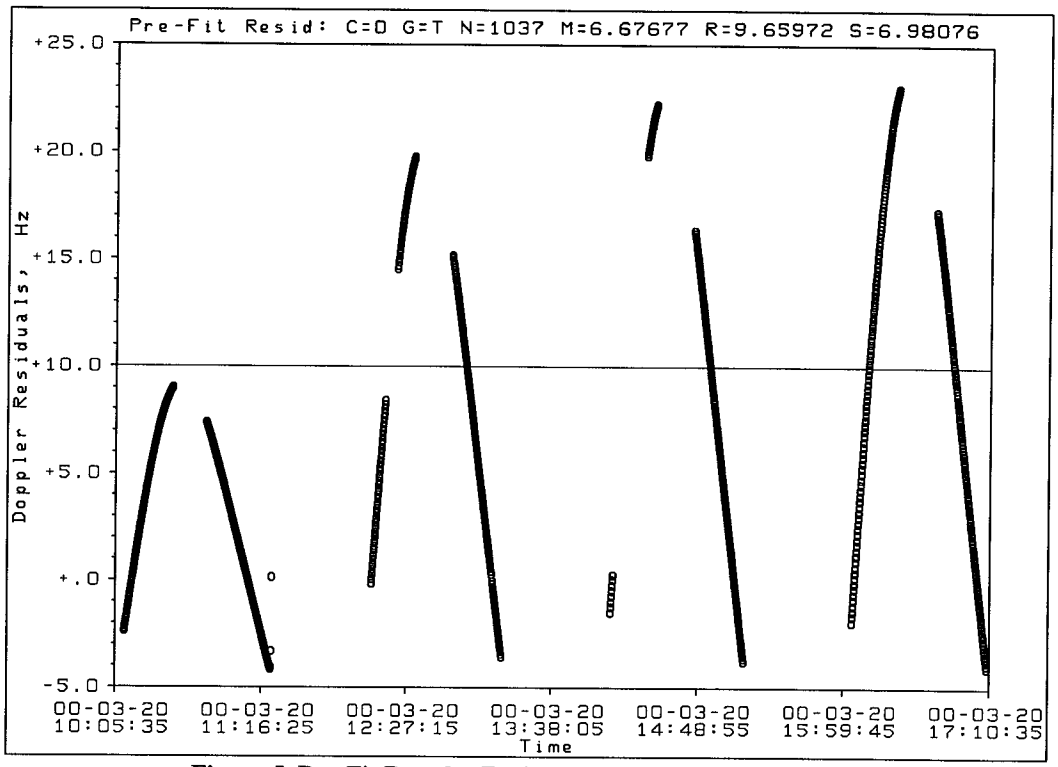

Figure 5 Pre-Fit Doppler Residuals For Prediction Analysis

Therefore, all of the previous solutions and residual plots must be reanalyzed. Looking at Figure 7, it is noted that there is a small trend in the residuals at the end of the second orbit. This trend was originally ignored for the following three reasons: (a) it is very small, (b) similar residual structure is not uncommon in the data analyses and is usually unrelated to AMDs, and (c) if this trend was due to an AMD, one would expect the remaining Doppler data not to fit this well. However, since an AMD modeled within the occultation period did not generate a good fit, and there seems no other place where an AMD could occur, a solution is generated with the AMD modeled at this time. The Doppler residuals turn out to be very good (Figure 9, sigma of 4.0 mHz), and the values of the estimated ΔV components are consistent with an accurate AMD epoch. Further analysis showed that the angle between the estimated AMD ΔV and the Earth LOS is 87.3 degrees. This is why very little of its effect is directly observed in the surrounding Doppler residuals.

When trying to fit the Doppler data without an AMD modeled, the filter has to try to reconcile the changed orbit (specifically the semi-major axis) after the AMD with the previous orbit. One can think of it as trying to determine an "average" orbit, resulting in the post-fit Doppler residuals being poor over the entire fit region. Also note that the inaccuracy of the initial modeling prohibits the detection of an AMD in the pre-fit residuals (Figure 5).

Another important item to note is that a good solution is required before all of the Doppler outliers can be detected and removed. For instance, in Figure 6 the most obvious Doppler outliers have been removed. However, there are still some segments of data which could be inaccurate and which could be contributing to the poor fit of the Doppler. One cannot be certain of the quality of these data until a better fit of the Doppler data is achieved, such as in Figures 8 and 9. Even in Figure 8 it is difficult to know if some data are accurate: the Doppler residuals at the end of orbit 1 and beginning of orbit 3 look like they could be inaccurate and causing the poor fit.

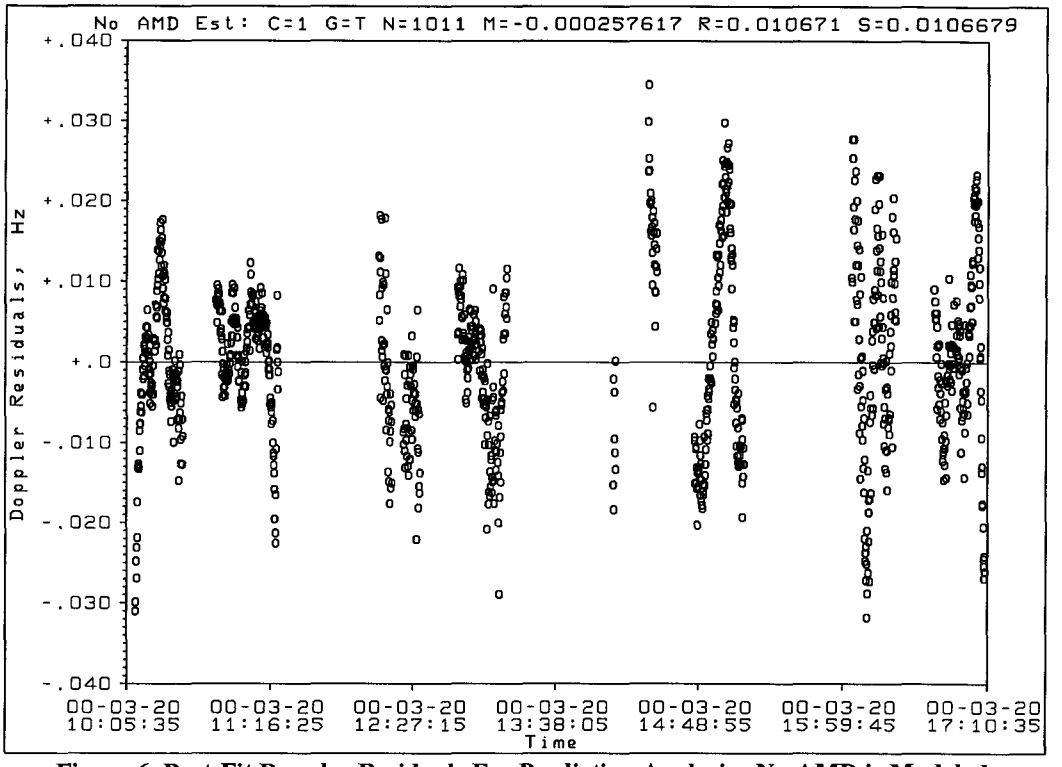

Figure 6 Post-Fit Doppler Residuals For Prediction Analysis. No AMD is Modeled.

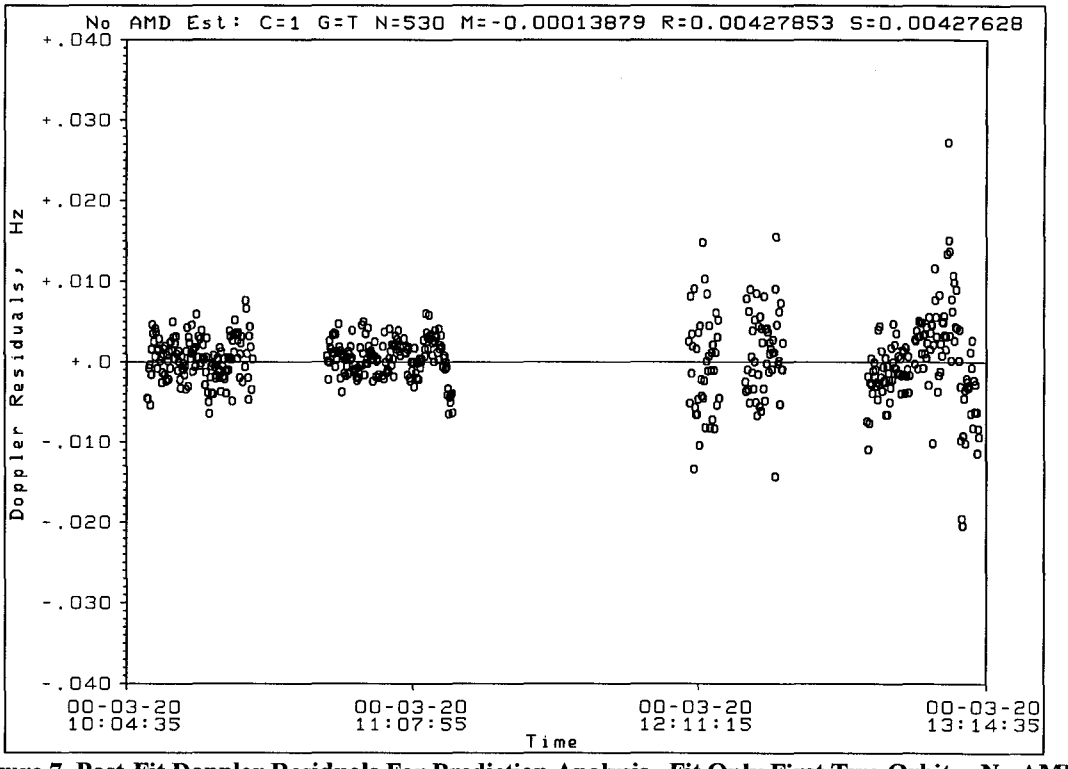

Figure 7 Post-Fit Doppler Residuals For Prediction Analysis. Fit Only First Two Orbits. No AMD Modeled.

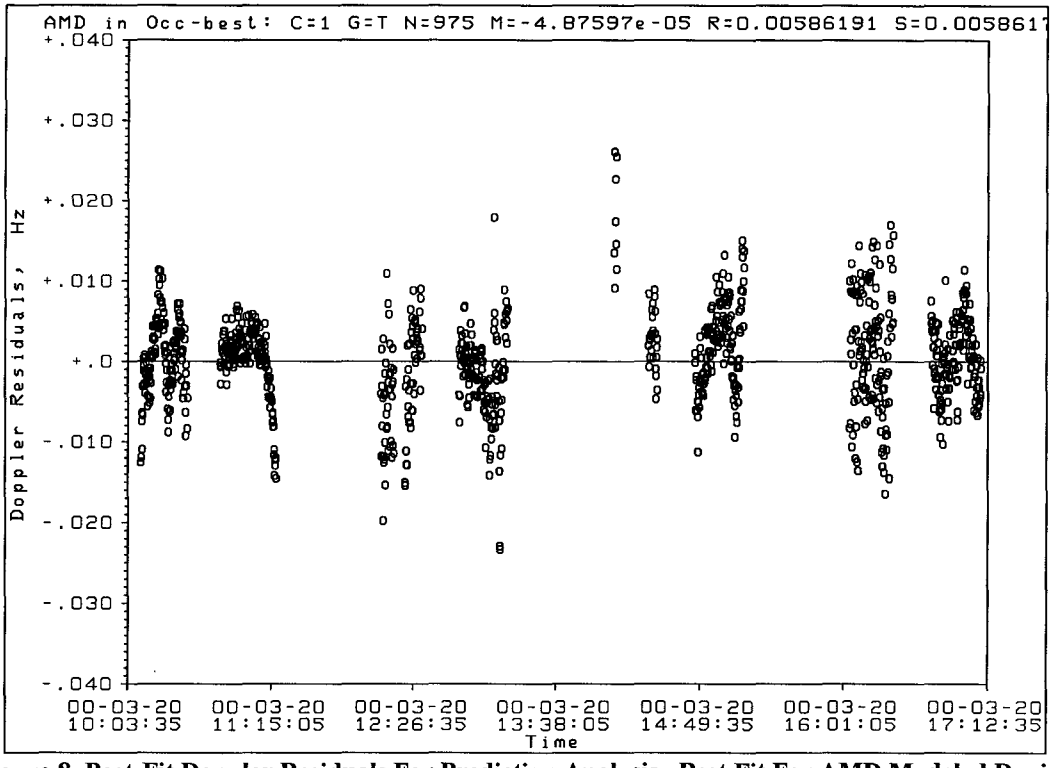

Figure 8 Post-Fit Doppler Residuals For Prediction Analysis. Best Fit For AMD Modeled During Occultation.

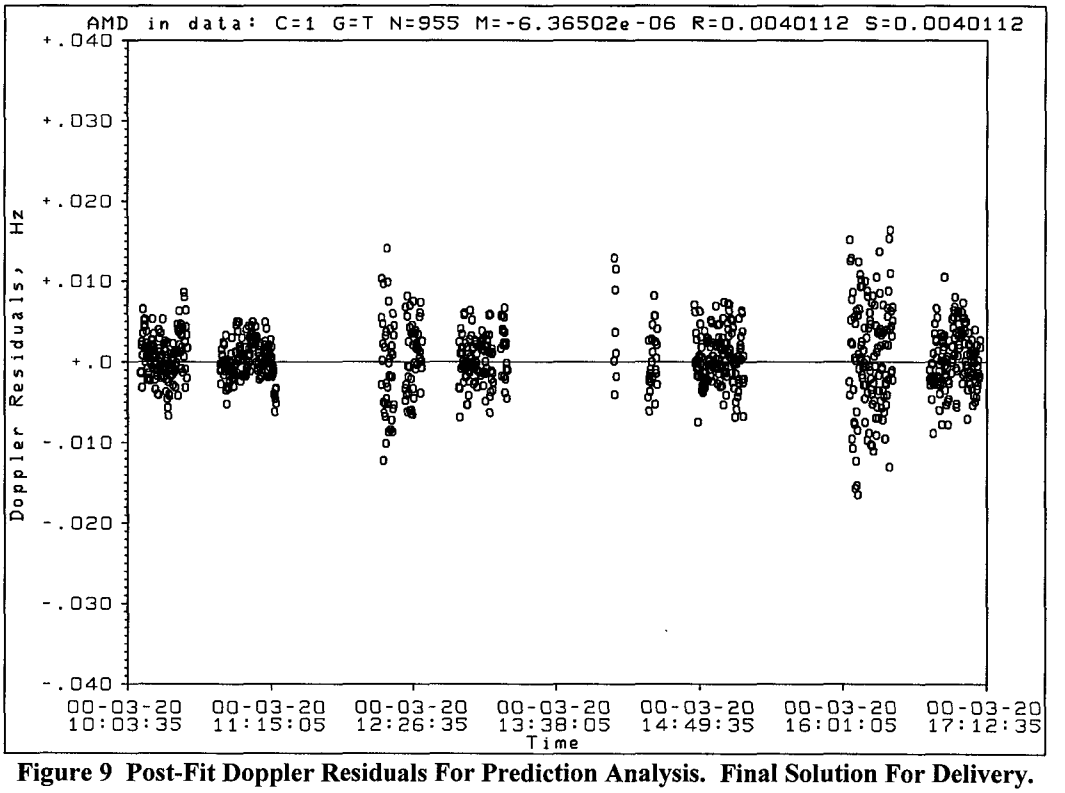

Figure 9 Post-Fit Doppler Residuals For Prediction Analysis. Final Solution For Delivery.

AMD Modeling for Prediction

Fitting the Doppler data is the first step in the generation of a prediction trajectory. After the OD solution has been generated, the trajectory has to be integrated several weeks into the future. The accuracy of the predicted trajectory depends on how closely the forces modeled in the integration correspond to the actual forces acting on the spacecraft. By far the largest contribution to this error is from the AMD mismodeling, which can cause a timing error near ten seconds after only a week of propagation. In a group of adjacent AMDs, each AMD often perturbs the spacecraft trajectory in a very different way. For instance, it is common to have one AMD cause the orbital period to decrease while the next one increases it. This perturbation in the period is caused by a small off nadir component of the AMD ΔV, which is difficult to model. As a result, even if the SCT could deliver predicted AMD information as accurate as their reconstructed AMDs (e.g. off nadir component of zero), this accuracy would not be sufficiently accurate to be of use in the predicted AMD modeling.

In many cases, though, the 1-2 day averaged effect of the AMDs on the trajectory remains nearly constant. A constant acceleration model can be used to simulate this average effect under the assumption that the AMD behavior will not change in the future. Prior to solar conjunction, Nav rarely attempted to model predicted AMDs as average accelerations. Due to changes in the AMD behavior, the majority of these attempts resulted in a worse prediction than if no acceleration was used. However, it became important to be able to generate accurate long-term predicted trajectories through the solar conjunction spacecraft command moratorium (6/25-7/7). Similar average AMD effects had been observed over the several weeks before conjunction, giving greater confidence that the future average AMD behavior would not be changing appreciably in the near term. Thus, Nav started to incorporate an acceleration model in the predicted trajectories. Although the AMD behavior did change significantly during solar conjunction, the acceleration model resulted in a more accurate prediction than if no such model had been included. After solar conjunction, the average AMD effect on the trajectory has been basically consistent, enabling Nav to incorporate more accurate acceleration models into its predictions. However, remember that the accuracies of these predictions depend on the AMD behavior remaining the same as in the recent past.

AMD Tabulation

Beginning in January 2000, NAV started to tabulate information on the AMDs with the goal that some insight might be gained into their effect on the trajectory. These tables consisted of: SCT delivered values of the AMDs, Nav estimated values of the AMDs, and the AMD effects on the spacecraft orbit (Figures 10-13). The following conclusions were reached: (a) the autonomous AMD unloading tended to occur at discrete true anomalies, (b) the SCT AMD ΔV magnitudes were 30-40% larger than the actual values derived by Nav directly from the Doppler data, (c) the AMDs appeared to have a small X component, contrary to the SCT's belief that an AMD should be entirely in the Z (nadir) direction (Figures 11, 12, 13), (d) the small AMD ΔVx was at least an order of magnitude smaller than the main ΔVz (Figures 10 and 13), (e) the trajectory timing errors were mainly due to this small ΔVx, (f) an AMD could cause negative or positive changes in the semi-major axis or orbit period, resulting in positive or negative timing errors (Figure 12), and (g) the AMDs during a 2-day time span generally cause both positive and negative changes in the semi-major axis - the timing errors seen in the predictions are an accumulation of these effects.

Generally, AMDs occur autonomously when the reaction wheel angular momentum exceeds a nominal threshold of 10 Nms. Since the time between spin-axis AMDs can vary by several hours, one would expect them to occur randomly around the orbit. However, they tend to occur near bands of true anomalies, and usually have similar ΔVx estimates at the same true anomaly. Since the HGA orientation can be correlated to the spacecraft true anomaly, this is one of the facts that support the theory that the off nadir AMD component is due to thruster impingement on the HGA.

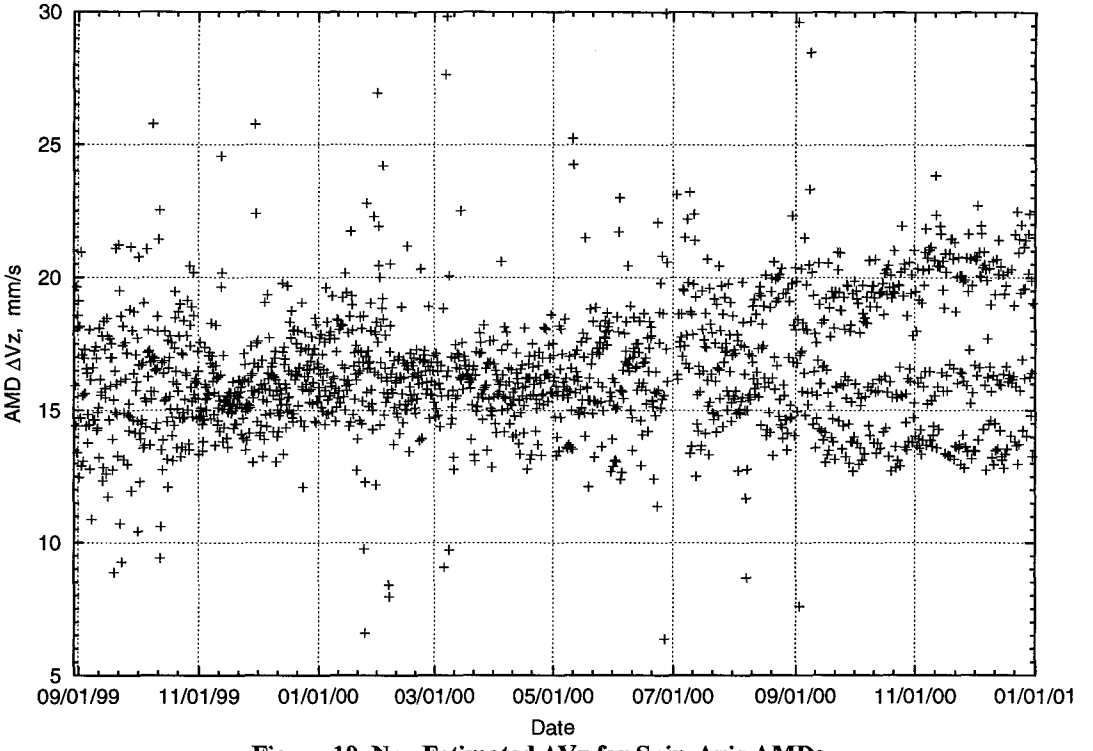

Figure 10 Nav Estimated ΔVz for Spin-Axis AMDs

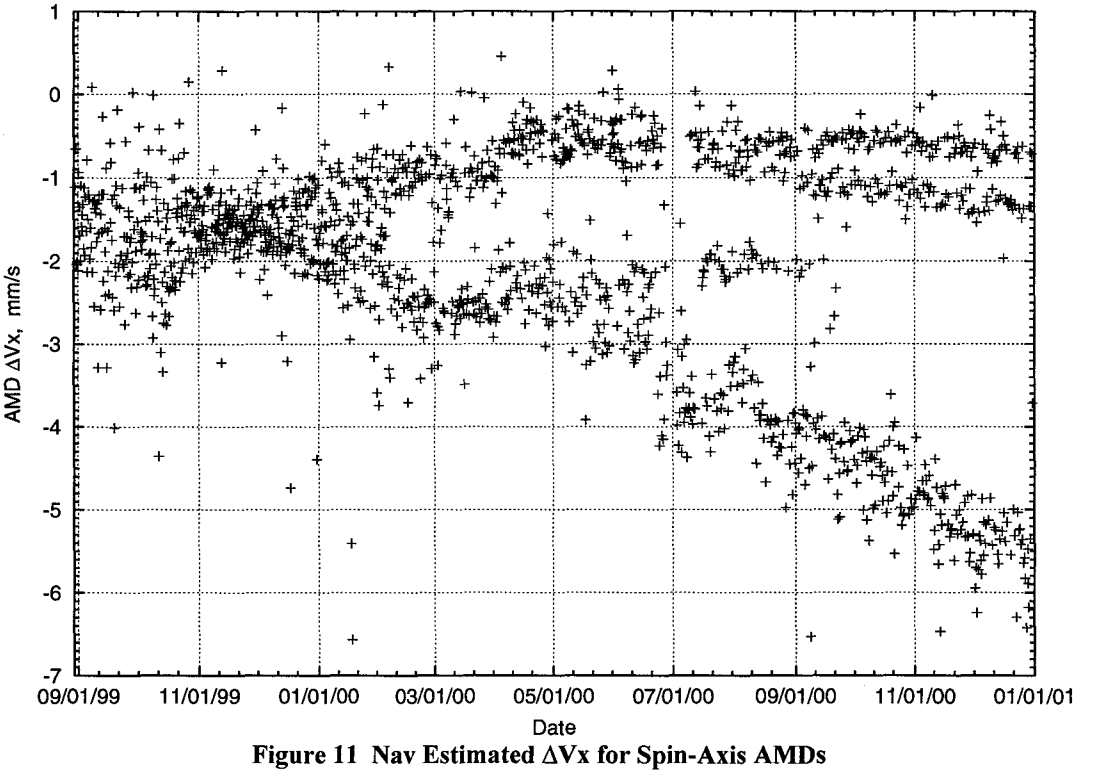

Figure 11 Nav Estimated ΔVx for Spin-Axis AMDs

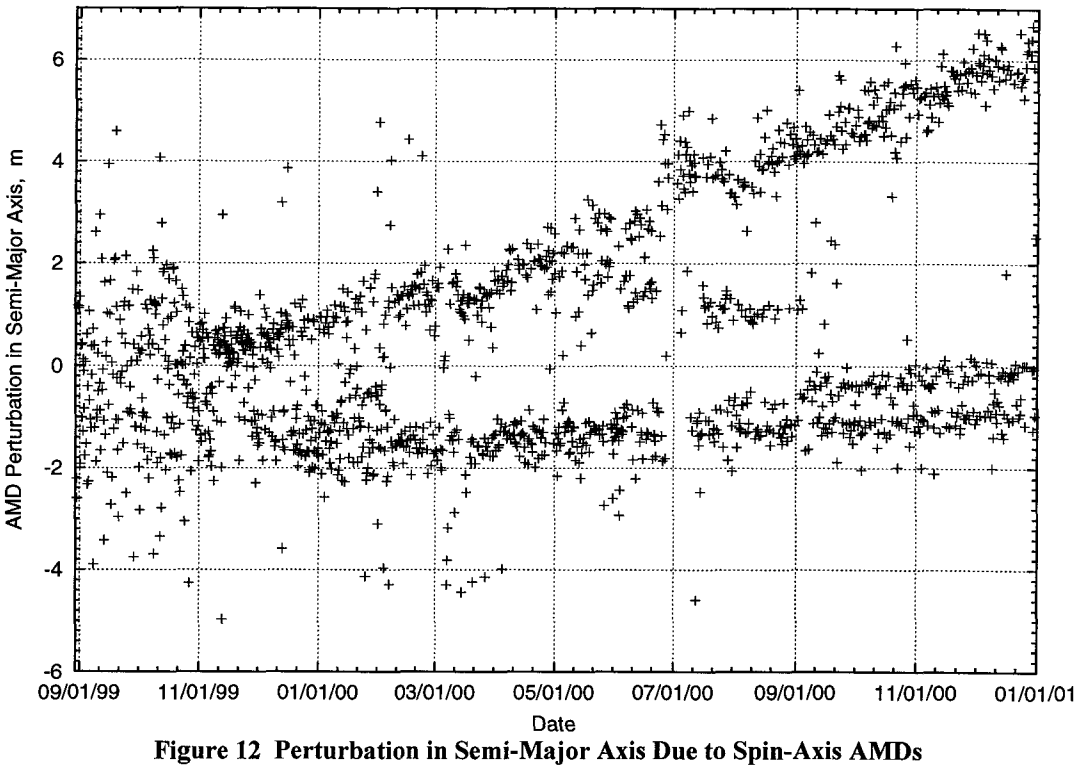

Figure 12 Perturbation in Semi-Major Axis Due to Spin-Axis AMDs

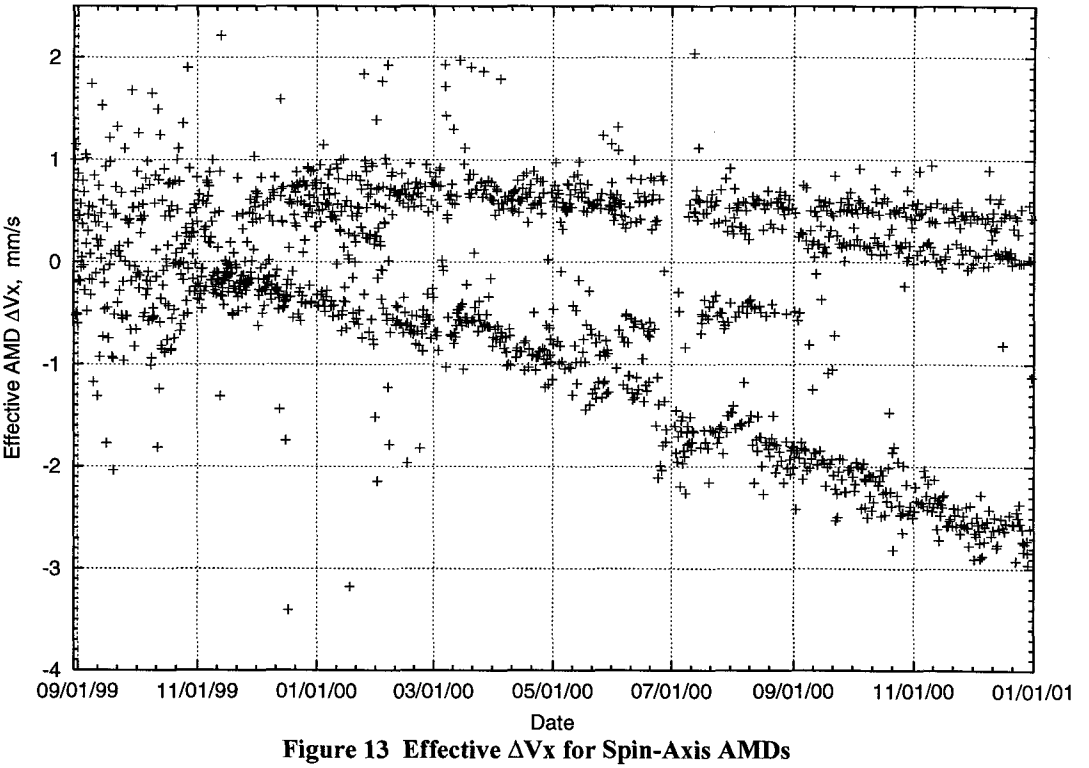

Figure 13 Effective ΔVx for Spin-Axis AMDs

By using the Doppler data to estimate for the AMD ΔV's, Nav was able to accurately determine the large Z-axis component of the AMDs. Figure 10 shows that a typical AMD has a ΔVz of around 17 mm/s. However, the values reported by the SCT in the AMD files are consistently 30-40% higher. The SCT reviewed the assumptions used in deriving their reconstructed AMDs and was able to improve their AMD ΔV values by 17%. All SCT AMD information delivered after August 27, 2000 at 16:00 UTC has included this correction. However, a discrepancy of 20% still exists and is unexplained.

Theoretically, the ΔV from an AMD should be along the spacecraft Z-axis since the spacecraft bus is nadir pointed. However, Nav has consistently found off nadir components. The off nadir component along the spacecraft Y-axis is small and appears to be random. The off nadir component along the spacecraft X-axis is larger and displays a bias (Figure 11). Part of this bias is an effect of the method Nav uses to model the AMD. After removing this modeling bias, there still exists a real, non-zero ΔVx. It was suspected that these off nadir AMD components are due to thruster plume impingement on the HGA, similar to what was observed during OTM-1. As mentioned above, this hypothesis is also supported by the correlation of the ΔVx values with the HGA orientation with respect to the thrusters. Analysis by the SCT, especially after solar conjunction, has supported this hypothesis.

To remove the bias in the AMD ΔVx, the method of modeling AMDs in the Nav process must be examined in more detail. An AMD is modeled as an instantaneous ΔV at the end of the AMD time span. However, the AMD has slightly perturbed the spacecraft position by this end time. Thus, a small change in the Z-axis position (ΔRz) is included in the AMD model to approximately account for this perturbation. Since the MGS spacecraft orbit is almost circular, it turns out that the semi-major axis (Figure 12) or period perturbation is a function of ΔRz and ΔVx. When an orbit is fit with the Doppler data, the filter just estimates for the ΔV that gives a good fit for the semi-major axis. Since ΔRz is not estimated, a different ΔRz causes the filter estimate of ΔVx to change so that the total effect on the semi-major axis and the trajectory is the same.

If the AMD is modeled as an instantaneous maneuver in the middle of the AMD time span, with no ΔR, then the filter estimate of ΔVx will be physically more realistic. A simple approximate equation can be used to convert the Nav ΔR and ΔV AMD model derived from a Doppler analysis into this alternative AMD model. Figure 13 shows the "effective" ΔVx derived from this equation, using the ΔRz from Figure 10 and the ΔVx from Figure 11. Note that the ΔVx estimates in Figure 11 are all negative. If these values were realistic, then the semi-major axis perturbations would always be positive, in contradiction with Figure 12. The effective ΔVx values in Figure 13, on the other hand, do imply semi-major axis perturbations similar to those in Figure 12.

Another important interpretation of Figures 12 and 13 is that the AMD perturbations on the trajectory are not consistent. They can generate either positive or negative changes in the semi-major axis. Before November 1999, the perturbations on the semi-major axis in Figure 19 looked like noise. The average effect of the AMDs, though, was to decrease the semi-major axis. Starting in November the semi-major axis perturbations separated into two distinct groups, one positive and the other negative. Less accurate gravity models and less mature solution strategies could have masked this effect before this time. After solar conjunction (July 1, 2000) the semi-major axis perturbations separated into three groups.

The long-term effect of the AMDs on the trajectory is an average of these positive and negative semi-major axis perturbations, which tend to cancel out, leaving only a small non-zero effect. For example, during September 2000, the average X-axis term of the acceleration model used for trajectory predictions was -0.025 $\mu m/s^2$. The equivalent average AMD ΔVx is only -0.67 mm/s, which changes the semi-major axis by +1.5 meters or the orbit period by 0.0042 seconds. These changes are three orders of magnitude smaller than the semi-major axis periodic perturbations due to the Mars gravity field at, for instance, periapsis.

Another benefit of this AMD table was to provide a long-term evolution of the AMD ΔV components, which enabled Nav to reduce the a priori uncertainties on the AMD components. This, in turn, minimized potential problems caused by unknown biases in the solution due to overly tight a priori constraints.

EFFECT OF GRAVITY FIELD MODELS ON ORBIT DETERMINATION

The other major error source in the orbit determination analyses is the Mars gravity field model (GFM), which not only affects the quality of the Doppler fit and the predicted trajectory, but also affects the modeling of other forces and the solution strategy. A less accurate gravity field produces larger Doppler residuals, which result in greater mismodeling of spacecraft dynamics. Less accurate modeling is magnified into larger errors in long trajectory predictions. For example, it is possible to have small aliasing between the gravity and AMD estimated parameters. The AMD ΔVx is relatively small and can be difficult to estimate accurately with a poor gravity field. So a small aliasing of the gravity field with ΔVx can cause an increasing degradation in the timing accuracy during the spacecraft trajectory propagation.

Less accurate modeling can also cause fundamental changes in the solution strategy. One such situation is when an AMD occurs near the end of the Doppler data arc (say within 20 minutes). Before Nav started using the MGS75C gravity field, it was found that it is better to cut off the data arc before the AMD. The resulting predicted trajectory was usually more accurate than if the data were fit through the AMD - even though this unmodeled AMD occurs right after the fit data and immediately perturbs the actual trajectory from the delivered predicted trajectory. On the other hand, if the MGS75C gravity field is being used the exact opposite is the case. A much better prediction is obtained if all the data past the AMD are fit, estimating for the AMD in the process.

The importance of an accurate gravity field is exhibited in the previous prediction analysis example. The effect of a gravity field model less accurate than MGS75C on the Doppler residuals is to slightly increase the random variation and add additional structure, usually in the form of frequent small oscillations. In Figure 9, the small AMD-related trend at the end of the second orbit would be undetectable. Even the significant residual structure in Figure 8 could be hidden. This illustrates why AMDs were often undetected or mismodeled in prediction analyses during the first several months of the mapping phase, especially when range data were unavailable.

Prior to the TMO maneuver, the navigation analysis utilized the Mars50c gravity model. The need for a more accurate gravity model led Nav to generate several "working" gravity fields using the gravity calibration tracking data. They were significant improvements over the Mars50c field and were used to design the TMO maneuver. Members of the radio science team at JPL were also creating improved gravity fields, which were periodically incorporated into the Nav analyses. Each gravity model improvement allowed Nav to generate better Doppler fits, reduce mismodeling, and generate better predictions. Due to the accuracy of the current MGS75C gravity model, the AMDs are now the major error source in all phases of the Nav analyses.

There are many strategies for examining the improvement in the gravity field models. From a navigation standpoint, a direct approach is to investigate the effect of different gravity fields on a typical Nav OD solution. Such an analysis was performed on the four orbits of data used in the example prediction analysis previously discussed. Several solutions were generated which were identical except for the nominal gravity field. Only the spacecraft state was estimated, with the nominal ΔV for the AMD being the one derived in the final solution (Figure 9).

The Doppler residuals give information on the accuracy of the gravity fields. A single parameter describing the quality of the residuals is the weighted "sum-of-squares" (SOS). Table 7 lists the SOS for each solution, the amount of MGS tracking data used to derive the gravity field and the date that the gravity field was incorporated into Nav analyses. This table shows that the gravity calibration period enabled Nav

to derive a gravity field which reduces the SOS by two orders of magnitude. Further refinements in the gravity field occurred over time, leading to the MGS75C field that is currently being used. This field shows an improvement of five orders of magnitude in the SOS over the original Mars50c gravity field. Additional information may be derived by examining plots of the residuals. The very large residuals with the Mars50C field (Figure 14) are reduced by an order of magnitude when the Nav preliminary gravity calibration field is used (Figure 15). These residuals are still large, though, and can be reduced by an additional order of magnitude using MGS75C. The resulting residuals are similar in magnitude to those in Figure 8 (sigma of 0.0087 Hz, variation between –0.02 Hz and 0.035 Hz), with structure similar to Figure 14. Note that a complete assessment of the quality of the gravity field models requires many different data arcs and analysis strategies.

Table 7

GRAVITY FIELD MODEL ASSESSMENT BASED ON DOPPLER DATA ANALYSIS

Gravity Field Model	Weighted Doppler Residuals SOS	Operational Date	Last MGS Data Analyzed for GFM*
Mars50c	20 776 955	MGS Aerobraking	--
Initial Nav Model	136 645	TMO Maneuver	2/9/99
Radio Science Interim	31 774	2/20/99	2/7/99
Radio Science Interim	1 495	4/01/99	2/28/99
MGS75B	2 044	6/22/99	3/29/99
MGS75C	372	12/15/99	11/8/99

* MGS data during the science phasing orbits were also used. Mariner 9 and Viking data were generally included, though MGS75C was derived from only MGS data. The Nav model was derived from 4.5 days of GC tracking data.

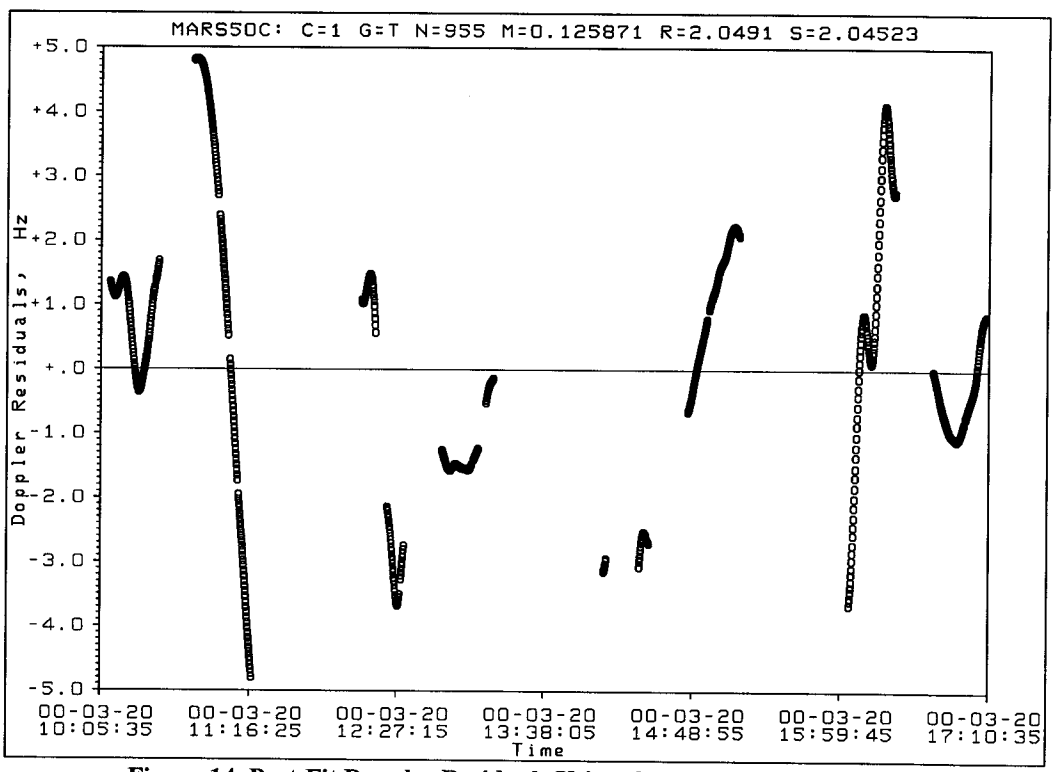

Figure 14 Post-Fit Doppler Residuals Using the Mars50c Gravity Field

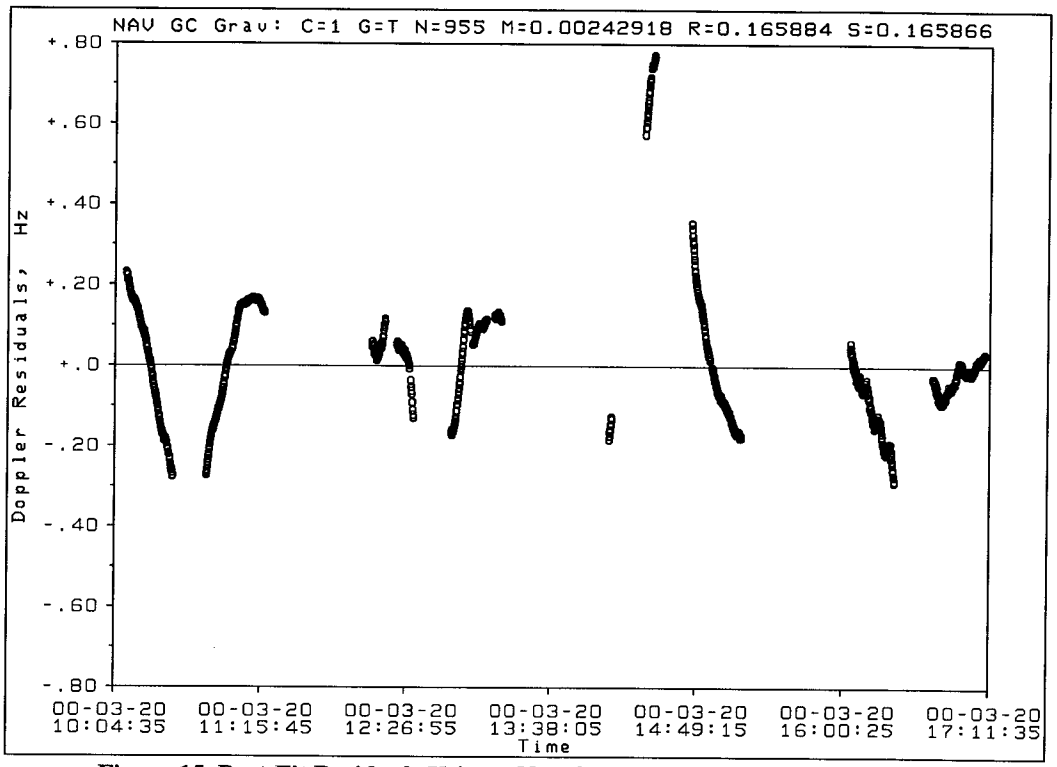

Figure 15 Post-Fit Residuals Using a Nav Gravity Calibration Gravity Field

CONCLUSIONS

The Navigation Team has processed Doppler data weekly for reconstructions and twice per week for predictions and generated spacecraft ephemerides over the entire 695 days of the mapping mission. Reconstruction position accuracies are generally better than 10 m, 200 m and 3 m, respectively, in the radial, down-track and cross-track directions. Within Doppler data arcs, these errors are reduced to 1 m, 50 m and 1 m, respectively. Prediction position errors after 20 days are typically better than 0.2 km, 70 km (20 sec) and 0.04 km, respectively, in the radial, down-track and cross-track directions.

The modeling of AMDs was the most challenging part of this analysis. Nav has analyzed over 3000 AMDs, of which 80 percent were spin-axis desaturations with an average ΔV magnitude of 17 mm/s. The AMD ΔVx values were small compared to the total ΔV perturbations, yet they were the major contributor to prediction timing errors. Due to the frequency stability of the USO, the majority of the one-way Doppler could be used for orbit determination. Range data were found to be valuable in the determination of AMDs in the prediction analyses.

ACKNOWLEDGEMENTS

The work described in this paper was carried out at the Jet Propulsion Laboratory, California Institute of Technology, under a contract with the National Aeronautics and Space Administration. The authors would like to acknowledge the contributions of the MGS project personnel, our LMA colleagues, especially Stuart Spath and Dave Eckart, the radio science team, especially William Sjogren and Dah-Ning Yuan, and the DSN for radiometric data aquisition.

REFERENCES

1. P. B. Esposito, V. Alwar, P. Burkhart, S. Demcak, E. Graat, M. Johnston, and B. Portock, "Navigating Mars Global Surveyor through the Martian Atmosphere: Aerobraking 2," AAS/AIAA Astrodynamics Specialist Conference, AAS-99-443, Girdwood, AK, August 16-19, 1999.

2. A. Konopliv and W. Sjogren, "The JPL Mars Gravity Field, Mars50c, Based Upon Viking and Mariner 9 Doppler Tracking Data," JPL Publication 95-5, Feb 1995.

3. D. Smith, et al, "The Gravity Field of Mars: Results from Mars Global Surveyor," Science, 286, pp. 94-97, 10/1/99. Also, W. L. Sjogren, private communication related to gravity field MGS75C, 1/4/2000.

4. B. Smith, "Antenna Problem Stalls Mars Mapping Mission, " Aviation Week and SpaceTechnology, p. 85, 26 April 1999.

5. A. Albee et al, "Overview of the Mars Global Surveyor Mission," JGR-Planets, publication date June, 2001.

6. C. Uphoff, "Orbit Selection for a Mars Geoscience/Climatology Orbiter," AIAA 22nd Aerospace Sciences Meeting, AIAA-84-0318, Reno, NV, January 9-12, 1984.

7. J. Neelon, S. Spath and W. Sidney, "Mars Global Surveyor Azimuth Gimbal Anomaly: The Analysis of the Problem and Solution and the Implementation," AAS/AIAA Space Flight Mechanics Meetimg, AAS 00-198, Clearwater, Florida, January 23-26, 2000.

8. ---, "Mars Observer Planetary Constants and Models," JPL Internal Document D-3444 (Project Document 642-321), November 1990.